Physics of the Earth and Planetary Interiors 275 (2018) 1–8

Contents lists available at ScienceDirect

Physics of the Earth and Planetary Interiors

journal homepage: www.elsevier.com/locate/pepi

Negative activation volume of oxygen self-diffusion in forsterite

Hongzhan Fei[a,b,*], Michael Wiedenbeck[c], Naoya Sakamoto[d], Hisayoshi Yurimoto[d], Takashi Yoshino[b], Daisuke Yamazaki[b], Tomoo Katsura[a]

[a] Bayerisches Geoinstitut, University of Bayreuth, Bayreuth D95440, Germany
[b] Institute for Study of the Earth's Interior, Okayama University, Misasa, Tottori 682-0193, Japan
[c] Deutsches GeoforschungsZentrum GFZ, Potsdam D14473, Germany
[d] Isotope Imaging Laboratory, Creative Research Institution, Hokkaido University, Sapporo 001-0021, Japan

ARTICLE INFO

Keywords:
Oxygen self-diffusion
Pressure dependence
Activation volume
Forsterite
Ionic conductivity
Upper mantle

ABSTRACT

Oxygen self-diffusion coefficients (D_{Ox}) were measured in single crystals of dry synthetic iron-free olivine (forsterite, Mg_2SiO_4) at a temperature of 1600 K and under pressures in the range 10^{-4} to 13 GPa, using a Kawai-type multi-anvil apparatus and an ambient pressure furnace. Diffusion profiles were obtained by secondary ion mass spectrometry operating in depth profiling mode. D_{Ox} in forsterite increases with increasing pressure with an activation volume of $-3.9 \pm 1.2\,cm^3$/mol. Although Mg is the fastest diffusing species in forsterite under low-pressure conditions, O is the fastest diffusing species at pressures greater than ~10 GPa. Si is the slowest throughout the stable pressure range of forsterite. Based on the observed positive and negative pressure dependence of D_{Ox} and D_{Mg} (Mg self-diffusion coefficient), respectively, $D_{Ox} + D_{Mg}$ in forsterite decreases with increasing pressure, and then increases slightly at pressures greater than 10 GPa. This behavior is in agreement with the pressure dependence of ionic conductivity in forsterite based on conductivity measurements (Yoshino et al., 2017), and can be used to explain the conductivity increase from ~300 km depth to the bottom of the asthenosphere.

1. Introduction

Atomic diffusion controls kinetic processes such as mineral grain growth, solid-state reactions, electrical conductivity, and high-temperature creep of minerals. Olivine [$(MgFe)_2SiO_4$] is thought to make up 60% of the volume of the Earth's upper mantle (Ringwood, 1991); thus, establishing the diffusion coefficients of elements in olivine is critical for understanding dynamic processes that occur in the Earth's upper mantle.

The self-diffusion coefficients of Mg and Si (D_{Mg} and D_{Si}, respectively), in iron-bearing olivine [$(MgFe)_2SiO_4$] and end-member forsterite (Mg_2SiO_4), as well as the inter-diffusion coefficient of Mg-Fe ($D_{Mg\text{-}Fe}$) in iron-bearing olivine, have been investigated systematically as functions of pressure, temperature, and water content (e.g., Fei et al., 2012, 2013, 2016; Farver and Yund, 2000; Jaoul et al., 1981; Andersson et al., 1989; Béjina et al., 1997, 1999, 2009; Houlier et al., 1988, 1990; Costa and Chakraborty, 2008; Dohmen et al., 2002a, 2007; Dohmen and Chakraborty 2007; Wang et al., 1999; Farver et al., 1994; Chakraborty, et al., 1994; Chakraborty, 1997; Hier-Majumder et al., 2005; Holzapfel et al., 2007; Jaoul et al., 1995; Bertran-Alvarez et al., 1992; Wang et al., 2004; Béjina et al., 2003; Chakraborty, 2010). There have also been a number of studies investigating the dependence of O self-diffusion on temperature, water content, and oxygen fugacity in forsterite and iron-bearing olivine (Sockel et al., 1980; Ando et al., 1981; Andersson et al., 1989; Costa and Chakraborty, 2008; Dohmen et al., 2002a; Fei et al., 2014; Gérard and Jaoul, 1989; Houlier et al., 1988; Jaoul et al., 1980; Reddy et al., 1980; Ryerson et al., 1989; Walker et al., 2003; Yurimoto et al., 1992). Despite these numerous studies, the pressure dependence of O self-diffusion (ΔV_{Ox}) remains poorly understood. Although Zhang et al. (2011) estimated ΔV_{Ox} for D_{Ox} in forsterite to be 17.1 cm^3/mol based on simulations using compensation law, experimental validation of the simulation is still needed.

In this study, we systematically measured D_{Ox} in single crystals of synthetic forsterite at 1600 K as a function of pressure in the range 10^{-4} (ambient pressure) to 13 GPa; a positive pressure dependence (i.e., a negative ΔV_{Ox}) is determined. This pressure dependence contrasts with

* Corresponding author at: Bayerisches Geoinstitut, University of Bayreuth, Bayreuth D95440, Germany.
E-mail address: hongzhan.fei@uni-bayreuth.de (H. Fei).

https://doi.org/10.1016/j.pepi.2017.12.005
Received 12 June 2016; Received in revised form 30 October 2017; Accepted 9 December 2017
Available online 19 December 2017
0031-9201/

the pressure dependence of Si and Mg diffusion, which have both been shown to be negative (Béjina et al., 2009; Chakraborty et al., 1994; Fei et al., 2012; Holzapfel et al., 2007).

2. Methods

The experimental methods used here will be described only briefly since they are in detail elsewhere (Fei et al., 2012, 2013, 2014). A single crystal of synthetic forsterite with no cracks nor optically visible inclusions, obtained from OXIDE Co., Mukawa, Japan, was used. The major impurity in the crystal was ~80 wt ppm of Ir, as determined by laser ablation inductively coupled plasma mass-spectrometry; this Ir impurity probably came from the capsule that was used during synthesis. Other trace elements were present with the following concentrations: Mn: ~3 wt ppm, Ni: ~2 wt ppm. Fe: ~2 wt ppm. Al: ~1.3 wt ppm, and others (Sc, Cr, Cu, Zn, Ga, Lu, Re, and Au) all with < 1 wt ppm (Fei et al., 2012).

In olivine, D_{Ox} has been found to be isotropic (Costa and Chakraborty, 2008; Jaoul et al., 1980). Therefore, D_{Ox} was only investigated along the *b* crystallographic axis in this study. Forsterite disks (1 mm diameter and 1 mm thickness) were cored along the *b*-axis from the initial single crystal. In order to protect the crystals from mechanical damage and to buffer the oxygen fugacity, each disk was loaded into a single-end sealed Pt capsule together with graphite powder. A small amount of enstatite ($MgSiO_3$) was mixed with the graphite powder to buffer the SiO_2 activity. Each capsule was dried in a vacuum furnace at 470 K for 24 h, and then sealed by arc welding on a hot plate. The Pt capsules, which contained the forsterite crystals, were then annealed at 1600 K and under pressures in the range 10^{-4} to 13 GPa for defect equilibrium. The ambient pressure experiments were performed using an ambient pressure furnace. The high-pressure experiments were performed using a Kawai-type multi-anvil apparatus with stepped-heater cell assembly design as illustrated in Fig. 1. Several 1 GPa experiments were performed using the experimental set-up described by Fei et al. (2012).

Pressure calibrations were performed at room temperature by phase transformation of Bi and ZnS, as well as at 1473 K by the olivine-wadsleyite transition in Mg_2SiO_4, with an uncertainty of ± 0.5 GPa. Although the defect equilibrium and diffusion experiments were performed at 1600 K, this temperature difference had a minimal effect on pressure because the pressure drop occurred at 500–1100 K during heating (displacement of the guide block of multi-anvil press rapidly

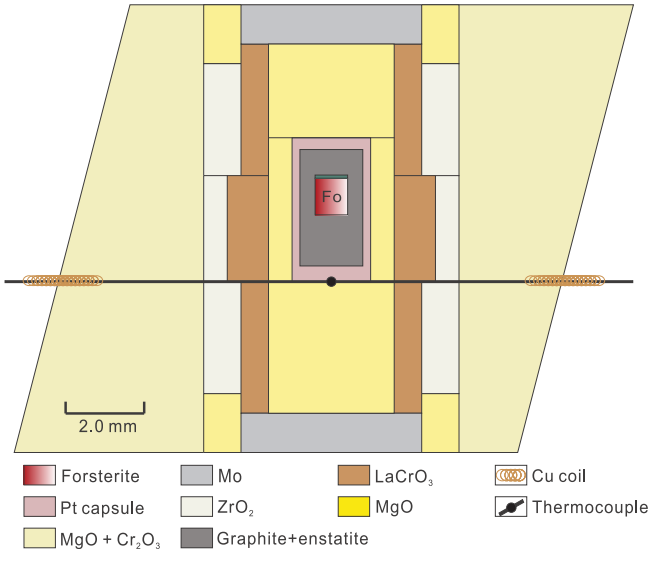

Fig. 1. Cross section of multi-anvil cell assembly that was used for high pressure experiments. (For interpretation of the references to colour in this figure legend, the reader is referred to the web version of this article.)

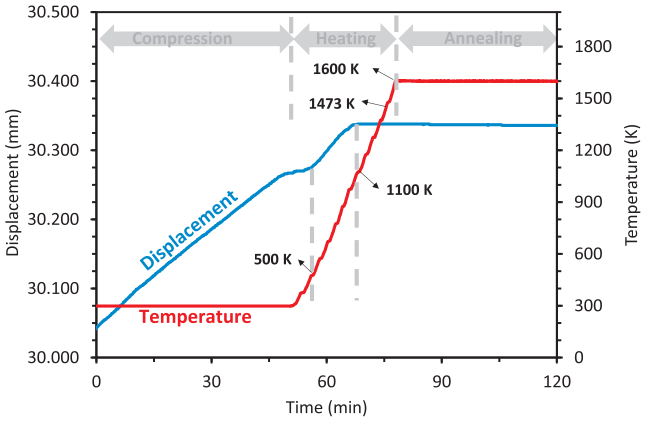

Fig. 2. An example of displacement of guide block during heating. The displacement increases sharply at 500–1100 K, indicating a pressure drop in the assembly. At above 1100 K and during annealing, the displacement remains approximately constant, indicating that there was no significant pressure change.

increased) (Fig. 2). At temperatures above 1100 K, the movement of guide block was negligible, such that no significant pressure change could be observed. The pressure was assumed to be constant during annealing by applying the constant tonnage on a constant volume of the assembly (displacement did not change significantly during annealing as shown in Fig. 2).

The temperature was continuously controlled during annealing using the auto-control function of Eurotherm-type device. The temperature gradient in the capsule was expected to be < 20 K/mm as reported by Shatskiy et al. (2007) for the same stepped-heater assembly. This temperature gradient has also been predicted by the simulations based on the thermal conductivities of the materials in the experimental assembly (Hernlund et al., 2006).

After defect equilibrium annealing, each disk was polished using a 0.25 μm diamond powder and an alkaline colloidal silica solution. A 300–500 nm thick ^{18}O-enriched Mg_2SiO_4 amorphous film was deposited on the surface using the pulsed laser deposition system at the Ruhr-University of Bochum (Dohmen et al., 2002b). An additional 100-

Table 1
Summary of experimental conditions and results for D_{Ox}. All experiments were performed at 1600 K. *P*: pressure, *t*: annealing duration. *Rs*: standard deviation of surface roughness measured at the bottom of SIMS crater by 3D-confocal microscope. D_{Ox}′: oxygen self-diffusion coefficient without roughness correction [no *L*(*Rs*) term for fitting in Eq. (1)]. D_{Ox}: oxygen self-diffusion coefficient after roughness correction.

Run. No.	*P* (GPa)	*t* (h)	*Rs* (nm)	D_{Ox}′ (m^2/s)	D_{Ox} (m^2/s)
S5045#1[a]	8	21	48	6.0×10^{-19}	5.9×10^{-19}
S5045#2[a]	8	21	61	7.6×10^{-19}	7.4×10^{-19}
V716#1[a,b]	8	52	162	1.4×10^{-18}	1.3×10^{-18}
V716#2[a,b]	8	52	128	2.4×10^{-18}	2.4×10^{-18}
D223#1	1	4.2	22	1.0×10^{-19}	6.3×10^{-20}
D223#2	1	4.2	12	7.6×10^{-20}	4.7×10^{-20}
D223#3	1	4.2	22	1.1×10^{-19}	7.1×10^{-20}
H3328#1	1	8	117	4.7×10^{-19}	2.8×10^{-19}
H3328#2	1	8	37	2.6×10^{-19}	2.3×10^{-19}
D220-2[b]	1	3.2	69	4.4×10^{-19}	2.6×10^{-19}
D225	1	15	40	6.7×10^{-20}	4.9×10^{-20}
F0021#1	10^{-4}	1	24	2.5×10^{-19}	8.6×10^{-20}
F0021#2	10^{-4}	1	33	2.8×10^{-19}	6.7×10^{-20}
F0022	10^{-4}	16	35	2.2×10^{-19}	2.0×10^{-19}
F0012	10^{-4}	50	115	6.6×10^{-20}	3.7×10^{-20}
F0010[b]	10^{-4}	12	20	1.2×10^{-19}	1.1×10^{-19}
5k2605B1	13	8	36	5.5×10^{-18}	5.5×10^{-18}
5k2605B2	13	8	54	2.6×10^{-18}	2.5×10^{-18}
5k2605T	13	8	58	2.5×10^{-18}	2.5×10^{-18}
5k2591	5	26	50	4.3×10^{-19}	4.2×10^{-19}

[a] Results of S5045 and V716 are already reported in Fei et al. (2014).
[b] Samples without ZrO_2 coating yielding the same D_{Ox} as those with ZrO_2 films.